Journal of Instrumentation

PAPER • OPEN ACCESS

Commissioning and first results of the 174 GHz collective Thomson scattering diagnostic at Wendelstein 7-X

To cite this article: D. Moseev *et al* 2024 *JINST* **19** C03056

Jinst

Published by IOP Publishing for Sissa Medialab

Received: *August 31, 2023*
Accepted: *October 16, 2023*
Published: *March 26, 2024*

20th International Symposium on Laser-Aided Plasma Diagnostics
Kyoto, Japan
10–14 September 2023

Commissioning and first results of the 174 GHz collective Thomson scattering diagnostic at Wendelstein 7-X

D. Moseev,[a,*] S. Ponomarenko,[a] H.P. Laqua,[a] T. Stange,[a] S.K. Nielsen,[b] H. Braune,[a] G. Gantenbein,[c] S. Illy,[c] J. Jelonnek,[c] W. Kasparek,[d] A. Kuleshov,[e] L. Krier,[c,a] C. Lechte,[d] S. Marsen,[a] M. Nishiura,[f] B. Plaum,[d] R. Ragona,[b] T. Ruess,[c] M. Salewski,[b] P. Stordiau,[g] M. Thumm,[c] R.C. Wolf,[a] J. Zimmermann[a] and the W7-X Team

[a] *Max-Planck-Institut für Plasmaphysik, Wendelsteinstr. 1, 17493 Greifswald, Germany*
[b] *Department of Physics,Technical University of Denmark, Fysikvej Building 309, DK-2800 Kgs. Lyngby, Denmark*
[c] *Institute for Pulsed Power and Microwave Technology, Karlsruhe Institute of Technology, Hermann-von-Helmholtz Platz 1, Buidling 421, 76344 Eggenstein-Leopoldshafen, Germany*
[d] *Institut für Grenzflächenverfahrenstechnik und Plasmatechnologie, Stuttgart University, Pfaffenwaldring 31, 70569 Stuttgart, Germany*
[e] *Vacuum Electronics Department, O.Ya. Usikov Institute for Radiophysics and Electronics, Akademika Proskury St. 12, 61085 Kharkiv, Ukraine*
[f] *National Institute for Fusion Science, 322-6 Oroshi, Toki, Gifu 509-5292, Japan*
[g] *Department of Applied Physics, Technical University of Eindhoven, De Groene Loper 19, 5612 AP Eindhoven, Netherlands*

E-mail: dmitry.moseev@ipp.mpg.de

Abstract: Collective Thomson Scattering (CTS) diagnostics measure the scattering spectrum of monochromatic incident radiation off collective fluctuations in the plasma. In this contribution, we present the first results from the upgraded CTS diagnostic at Wendelstein 7-X (W7-X) operating in the frequency range between 172 and 176 GHz. This frequency range allows for minimization of noise originating from the electron cyclotron emission in the plasma. Consequently, the good signal-to-noise ratio allows measurements of fast ions or bulk plasma parameters with higher temporal resolution compared with the previously used 140 GHz system.

Keywords: Microwave radiometers; Microwave Antennas

*Corresponding author.

https://doi.org/10.1088/1748-0221/19/03/C03056

2024 JINST 19 C03056

Contents

1 Introduction

Collective Thomson scattering (CTS) diagnostic is used for diagnosing collective fluctuations in plasmas caused by ion motion, turbulence or plasma waves. A high-power microwave beam or laser beam is sent into the plasma, where it scatters off electrons. The collective regime of Thomson scattering is defined by the characteristic length of resolved perturbation. If the resolved wave vector $\mathbf{k}_\delta = \mathbf{k_s} - \mathbf{k_i}$, where $\mathbf{k_i}$ and $\mathbf{k_s}$ stand for the wave vectors of incident and received scattering radiation, respectively, exceeds the inversed Debye length, the scattering is incoherent. Otherwise it is collective (coherent) Thomson scattering. This is expressed by the Salpeter parameter [1], which should be much greater than one for the collective regime:

$$\alpha = \frac{1}{k_\delta \lambda_D} > 1, \tag{1.1}$$

where α is the Salpeter parameter and λ_D is the Debye length.

The diagnostic aimed at fast ion research operated at TFTR [2], ASDEX Upgrade [3–5], TEXTOR [6, 7], LHD [8, 9], W7-AS [10, 11], GDT [12, 13], and will be installed at ITER [14]. The diagnostic is sensitive to the projection of the ion velocity distribution function on the direction of $\mathbf{k}_\delta$ [15]. Having prior knowledge about the shape of the distribution function (e.g. (drifted bi-) Maxwellian, slowing down distribution, ring distribution, etc [16]) and combining CTS measurements with other fast ion diagnostics enables reconstruction of the complete velocity distribution function [17–20].

Initially, the CTS diagnostic at W7-X was designed for ion temperature (T_i) measurements using one of the heating gyrotrons as a source of probing radiation [21, 22]. The diagnostic delivered ion temperature, however poor signal-to-noise ratio (SNR) due to strong electron cyclotron emission (ECE) in the order of several keV required long averaging. Another drawback of using a heating gyrotron as a source of probing radiation is that the measurement volume cannot be placed behind or even near the electron cyclotron resonance layer for the chosen frequency range.

2024 JINST 19 C03056

Consequently, a new frequency range for the diagnostic was selected based on the following criteria:

- Low ECE power density,
- Technical capability of detuning existing heating gyrotrons to the new frequency,
- Low reflections from diamond discs that are used as air-vacuum interfaces in gyrotrons and in the plasma vessel.

We showed, that the optimal frequency range is 171–177 GHz [22]. Indeed, this range is located between the second and third harmonic of ECE coming from the plasma [23]. Theoretical investigation showed that existing gyrotrons could emit microwave pulses of several ms particularly at a frequency of 174 GHz, should their magnets be replaced to those which can deliver around 7.1 T instead of currently used 5.6 T [24]. The prediction was proven experimentally. Additionally, we showed that the frequency drift of the high-power gyrotron could be stabilized [25] which allows CTS measurements with a narrow notch filter.

We upgraded the CTS receiver to the new frequency range by exchanging a 140 GHz corrugated microwave horn with a smooth dual-frequency horn for the 140 and 174 GHz ranges. The horn is followed by a waveguide switch which redirects scattering radiation either into the 140 GHz radiometer or into the 174 GHz radiometer. Two key features of the new receiver are single-stage heterodyne in contrast to the two-stage mixing in the 140 GHz arm and a new radiofrequency (RF) amplifier from ELVA-1 with the gain of 14 dB and noise figure of 8 dB in the 170–180 GHz frequency range. These improvements lowered the noise temperature of the 174 GHz CTS receiver to around 2 eV down from around 8 eV for the 140 GHz case. A detailed characterization of the new receiver is reported separately [26].

This paper is organized as following. In section 2 we discuss the operational implications of the diagnostic working at 174 GHz. The overlap sweep is shown in section 3. We discuss the properties of thermal and fast ion signatures in the measured CTS spectra in sections 4 and 5, respectively. Section 6 concludes the paper.

2 Implications of the 174 GHz probing radiation

The main advantage of the CTS diagnostic in the 174 GHz frequency range is that this range is located exactly in between the second and third harmonics of ECE for plasmas confined within the last closed flux surface, which means minimum possible noise from ECE in the measurements. However, it also means that the microwave radiation is only weakly absorbed by the plasma. Corre et al. showed [27] that direct irradiation of a graphite tile with a 140 GHz beam having an average unabsorbed power of 240 kW led to a temperature increase of the impacted tile to almost 1000 °C. Moreover, the thermodynamic equilibrium was not achieved within 10 s of the discharge 20171121.13. The same power is extracted from the gyrotron at 174 GHz during the CTS operation. Unabsorbed microwave power in the 174 GHz frequency range is potentially harmfull for other microwave diagnostics which are not equipped with notch filters for 174 GHz. This problem is not yet solved. In commissioning experiments discussed in this paper, the shutters of all potentially endangered diagnostics were closed. In the future they will be equipped with notch filters for the 174 GHz radiation or fast irises if installation of a notch filter for some reason is impossible.

2024 JINST 19 C03056

The CW operation of the 140 GHz gyrotron at 174 GHz has implications not only for W7-X but for the gyrotron itself. The efficiency of the gyrotron is down from around 45% to about 15%. This means that the thermal loads on the collector from the electron beam increase by more than 50%. The gyrotron also produces far more stray radiation because the microwave launcher in the device is only optimized to convert the $TE_{28,8}$ mode into a Gaussian beam. The conversion efficiency of other modes is lower, as discussed in ref. [24]. High fluxes of stray radiation inside the gyrotron can lead to damages.

Considering these factors, we chose to operate the gyrotron at a duty cycle of 7%, 10 ms on and 130 ms off as it is shown in figure 1. The CTS measurements lasted 3 ms during the gyrotron-on period, it was followed by a 3 ms ECE background measurement right after the gyrotron was turned off. The sequence was repeated every 140 ms.

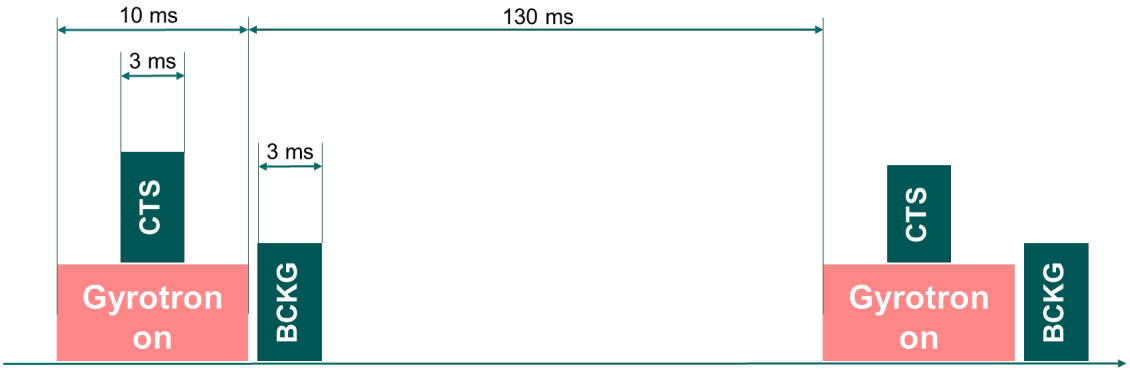

Figure 1. Timing of the gyrotron and data acquisiton in the CTS experiments.

3 Overlap sweep

One of the main validity proofs of CTS measurements is an overlap sweep, when the receiver beam is swept across the probing beam. The scattering should take place only when two beams intersect, so a bell-like shape of an integrated spectral power density as a function of the sweeping angle (or time) is expected, should the received signal indeed originate from scattering.

A schematic of the overlap sweep in the shot 20230323.14 is shown in figure 2. The receiver beam F1 is swept across the probing beam B1, which shines nearly perpendicular to the first wall, slightly bent to the right. The receiver beam is swept from left to right and stopped at the final location. Reflections of the probing beam B1 in such a configuration create secondary overlaps futher on the right from beam B1.

On the left panel of figure 3 we demonstrate an integrated power spectral density (PSD) of the lower frequency wing of the scattering spectra as a function of time during the discharge 20230323.14. On the right panel of figure 3 the expected normalized PSD as a function of the receiver scanning angle is plotted. The difference between the two is clear:

- The integrated spectra are never zero during the sweep;
- Values of integrated spectra do not fall back to the initial values in the beginning of the overlap sweep.

2024 JINST 19 C03056

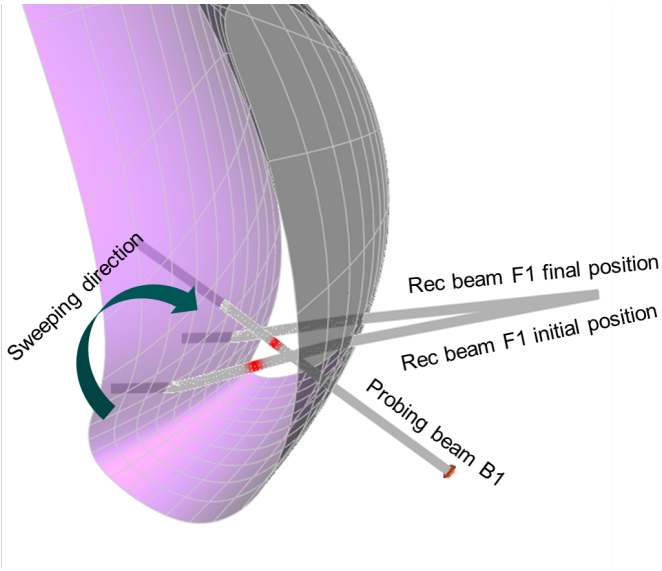

Figure 2. Schematic of the overlap sweep of the receiver beam F1 across the probing beam B1 in the W7-X experiment 20230323.14.

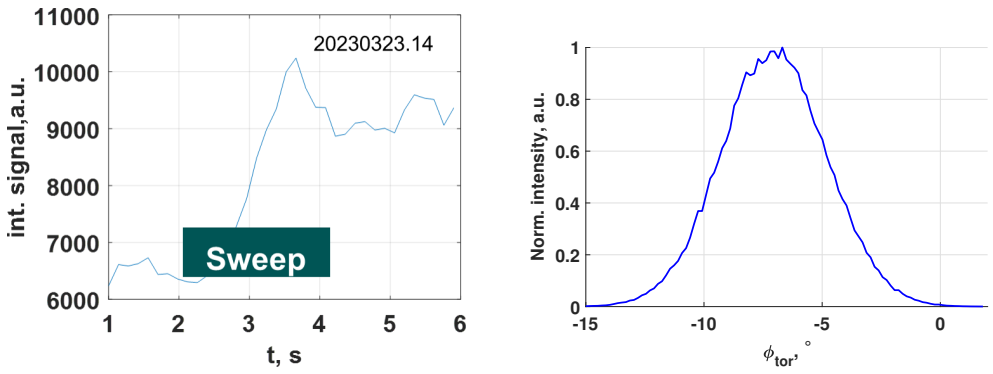

Figure 3. Left panel: integrated low frequency wing of the CTS spectra as a function of time during an overlap sweep of the CTS receiver across the probing beam in the W7-X experiment 20230323.14. Right panel: expected shape of integrated CTS spectra as a function of the scanning angle.

The ECE background never goes to zero and remains in the range 20–70 eV [23, 26]. During the gyrotron-on period a process of slight absorption of the 174 GHz probing beam and re-emission in a broader spectral range takes place at the plasma edge. Consequently, the background subtraction always leaves an offset in the spectrum and that is why the integrated PSD of the scattering spectra during the overlap sweep never reaches zero.

Secondary overlaps from the reflected probing beam explain a slight decrease of the integrated signal at the end of the overlap sweep compare to its maximum. For the next campaign a diffusor structure will be milled into the impacted first wall tile in order to dissipate the probing beam into all direction after the first reflection.

2024 JINST 19 C03056

4 Thermal CTS spectra

It is important to see how much of an improvement the transition to the new frequency and re-design of the receiver really helps to improve SNR, as shown in figure 4. Frequencies on both panels are relative to frequencies of the probing beams. On the left panel one sees two normalized CTS spectra from the W7-X discharge 20171011.53, when the CTS diagnostic operated at 140 GHz. The blue curve is obtained by averaging over a single gyrotron pulse (5 ms). SNR of such a spectrum is poor and the spectrum is not useful for T_i inference. The red line shows a spectrum averaged over 14 gyrotron pulses (70 ms) and T_i can be inferred from it [28], however temporal resolution is lost. Moreover, due to refraction, the exact position of the overlap volume has large uncertainties [22]. The right panel shows a normalized spectrum averaged in a single gyrotron pulse over 3 ms in the discharge 20230330.29. It has a good SNR allowing inference of not only the bulk plasma parameters but also of fast ions. One also notices a narrow notch filter compare to the 140 GHz case shown on the left panel, low refraction, and availability of plasma center, a location previously unavailable due to the location of the ECRH absorption layer for measurements.

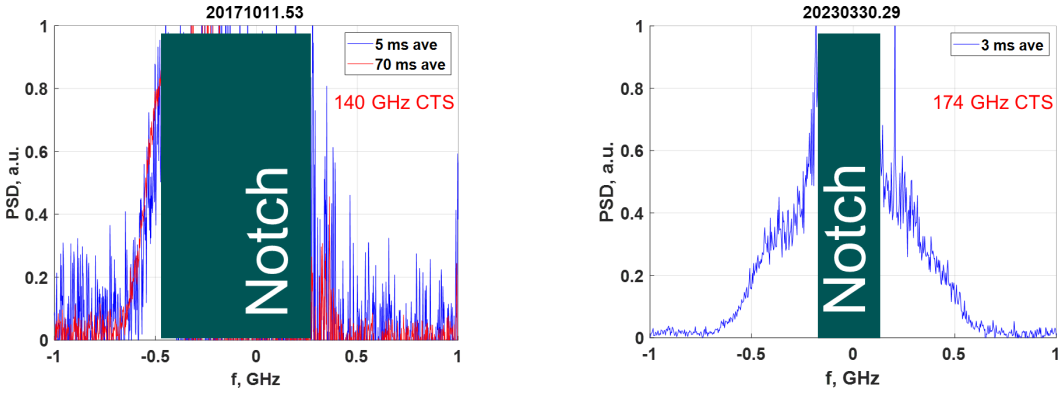

Figure 4. Left panel: two scattering spectra for T_i measurements from the W7-X dischargre 20171011.53 obtained with the 5 ms averaging (over a single gyrotron pulse, blue curve) and with 70 ms averaging (over 14 gyrotron pulses, red curve). Right panel: a scattering spectrum for T_i measurements from the W7-X discharge 20230330.29 averaged over 3 ms (single gyrotron pulse). Both panels show normalized spectra and frequency relative to the frequency of the source of the probing beam.

5 Fast ion measurements

W7-X is equipped with four neutral beam injectors (NBI), 55 keV 1.8 MW each, which in future will be expanded to eight sources [29]. The discharge 20230323.38 is shown in figure 5, where a single neutral beam injector S4 fired for 5 s, as seen on the upper panel. Since we do not have an absolute calibration of the CTS receiver due to an urgent repair, we instead demonstrate the effect of fast ions as follows. The CTS measurements were made throughout the discharge. A ratio of two CTS spectra is shown on the lower panel. One taken during the NBI phase 28 ms before the injector was switched off (PSD_{NBI}), over the spectrum taken 12 ms after NBI turned off (PSD_{noNBI}). The moments when the spectra are taken are indicated by black and magenta vertical lines on the upper panel. Each of the measured spectra has three large contributions, namely ECE, thermal ion spectra,

2024 JINST 19 C03056

and the fast ion spectrum:

$$R = \frac{\mathrm{PSD}^{\mathrm{ECE}}_{\mathrm{NBI}} + \mathrm{PSD}^{\mathrm{thermal}}_{\mathrm{NBI}} + \mathrm{PSD}^{\mathrm{FI}}_{\mathrm{NBI}}}{\mathrm{PSD}^{\mathrm{ECE}}_{\mathrm{noNBI}} + \mathrm{PSD}^{\mathrm{thermal}}_{\mathrm{noNBI}} + \mathrm{PSD}^{\mathrm{FI}}_{\mathrm{noNBI}}}, \tag{5.1}$$

where R denotes the ratio, PSD is the power spectral density of the respective contribution which is indicated in superscript. The phase of the discharge when the measurement was done is shown in the subscript. It is important to emphasize that by ECE we do not mean the total ECE in the frequency range but rather its increment during the 174 GHz gyrotron-on phase which cannot be removed by background subtraction. The ECE increment is flat in our frequency range and typically accounts for 20–30 eV. The thermal part of the spectra spans ±500–700 MHz from the probing frequency and is not expected to change between the two different phases. This is because 12 ms in the new discharge phase, when the reference spectrum was taken, is an order of magnitude smaller than the energy (200 ms) and particle (500 ms) confinement times. The fast ion feature of 55 keV hydrogen ions is supposed to give a spectral response in the range ±1500 MHz from the probing frequency [22]. Due to the close to perpendicular CTS viewing geometry and close to radial NBI injection geometry, no strong asymmetries in the fast ion spectral feature are expected.

Indeed, what we observe in figure 5 is an elevated ratio R between the two spectra by about 5% in the ±1300 MHz from the probing frequency. With no fast ion signatures we would expect, disregarding the noise, the ratio curve to be flat with a value of 1. The lowering of the ratio R shows where the bulk thermal spectrum is and how the fast ion signature gets weak compare to it. Knowing our usual ECE levels, the fast ion signature is estimated to be at a level of 1–1.5 eV.

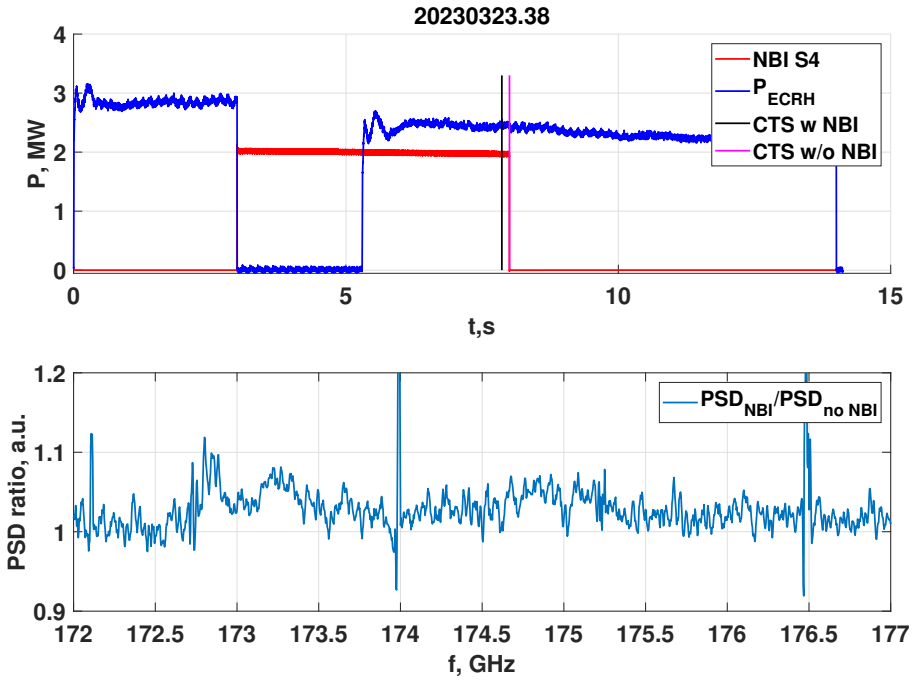

Figure 5. Upper panel: time traces of NBI and ECRH heating in discharge 20230323.38. The moments of the CTS measurements are marked by vertical black (NBI phase) and magenta (no NBI phase) lines. Lower panel: ratio R between the CTS spectra in the NBI and no-NBI phases of the discharge.

2024 JINST 19 C03056

6 Conclusions

The CTS diagnostic at W7-X, including the receiver and the probing gyrotron, were modified to measure around a probing frequency of 174 GHz. The modifications led to an improvement in the amount of ECE noise that enters the receiver. The performance of the receiver itself was improved by using a D-band RF amplifier, a single heterodyne architecture, and a narrow notch filter in combination with the frequency-stabilized gyrotron.

The diagnostic acquires high quality spectra with SNR good enough to allow for both bulk ion and fast ion measurements with a 3 ms time resolution.

Special protection measures for other RF diagnostics have to be implemented in order integrate the CTS diagnostic into the set of standard operation diagnostics of W7-X.

Acknowledgments

This work has been carried out within the framework of the EUROfusion Consortium, funded by the European Union via the Euroatom Research and Training Programme (Grant Agreement No 101052200 — EUROfusion). Views and opinions expressed are however those of the author(s) only and do not necessarily reflect those of the European Union or the European Commission. Neither the European Union nor the European Commission can be held responsible for them.

References

[1] E.E. Salpeter, *Electron Density Fluctuations in a Plasma*, *Phys. Rev.* **120** (1960) 1528.

[2] J.S. Machuzak et al., *Results from the low-power 60 GHz gyrotron collective Thomson scattering diagnostic on TFTR*, *Rev. Sci. Instrum.* **68** (1997) 458.

[3] M. Salewski et al., *Comparison of fast ion collective Thomson scattering measurements at ASDEX Upgrade with numerical simulations*, *Nucl. Fusion* **50** (2010) 035012.

[4] J. Rasmussen et al., *Consistency between real and synthetic fast-ion measurements at ASDEX Upgrade*, *Plasma Phys. Control. Fusion* **57** (2015) 075014.

[5] S.K. Nielsen et al., *Measurements of the fast-ion distribution function at ASDEX upgrade by collective Thomson scattering (CTS) using active and passive views*, *Plasma Phys. Control. Fusion* **57** (2015) 035009.

[6] H. Bindslev et al., *Fast-Ion Dynamics in the TEXTOR Tokamak Measured by Collective Thomson Scattering*, *Phys. Rev. Lett.* **97** (2006) 205005.

[7] S.K. Nielsen et al., *Temporal evolution of confined fast-ion velocity distributions measured by collective Thomson scattering in TEXTOR*, *Phys. Rev. E* **77** (2008) 016407.

[8] M. Nishiura et al., *Initial result of collective Thomson scattering using 77 GHz gyrotron for bulk and tail ion diagnostics in the Large Helical Device*, *J. Phys. Conf. Ser.* **227** (2010) 012014.

[9] M. Nishiura et al., *Spectrum response and analysis of 77 GHz band collective Thomson scattering diagnostic for bulk and fast ions in LHD plasmas*, *Nucl. Fusion* **54** (2014) 023006.

[10] E.V. Suvorov et al., *Ion temperature and beam-driven plasma waves from collective scattering of gyrotron radiation in W7-AS*, *Plasma Phys. Control. Fusion* **37** (1995) 1207.

2024 JINST 19 C03056

[11] A.G. Shalashov, E.V. Suvorov, L.V. Lubyako and H. Maassberg, *NBI-driven ion cyclotron instabilities at the W7-AS stellarator*, *Plasma Phys. Control. Fusion* **45** (2003) 395.

[12] A.G. Shalashov et al., *First results of collective Thomson scattering diagnostic of fast ions at the GDT open magnetic trap*, *Phys. Plasmas* **29** (2022) 80702.

[13] A.G. Shalashov et al., *Development of fast-ion collective Thomson scattering diagnostics for the GDT experiment*, 2021 *JINST* **16** P07007.

[14] S.B. Korsholm et al., *ITER collective Thomson scattering — Preparing to diagnose fusion-born alpha particles (invited)*, *Rev. Sci. Instrum.* **93** (2022) 103539.

[15] M. Salewski et al., *On velocity space interrogation regions of fast-ion collective Thomson scattering at ITER*, *Nucl. Fusion* **51** (2011) 083014.

[16] D. Moseev and M. Salewski, *Bi-Maxwellian, slowing-down, and ring velocity distributions of fast ions in magnetized plasmas*, *Phys. Plasmas* **26** (2019) 020901.

[17] D. Moseev et al., *Recent progress in fast-ion diagnostics for magnetically confined plasmas*, *Reviews of Modern Plasma Physics* **2** (2018) 7.

[18] M. Salewski et al., *Measurement of a 2D fast-ion velocity distribution function by tomographic inversion of fast-ion D-alpha spectra*, *Nucl. Fusion* **54** (2014) 023005.

[19] B.S. Schmidt et al., *4D and 5D phase-space tomography using slowing-down physics regularization*, *Nucl. Fusion* **63** (2023) 076016.

[20] B. Madsen et al., *Fast-ion velocity-space tomography using slowing-down regularization in EAST plasmas with co- and counter-current neutral beam injection*, *Plasma Phys. Control. Fusion* **62** (2020) 115019.

[21] I. Abramovic et al., *Forward modeling of collective Thomson scattering for Wendelstein 7-X plasmas: Electrostatic approximation*, *Rev. Sci. Instrum.* **90** (2019) 023501.

[22] D. Moseev et al., *Collective Thomson Scattering Diagnostic for Wendelstein 7-X at 175 GHz*, 2020 *JINST* **15** C05035.

[23] N. Chaudhary et al., *Investigation of higher harmonics of electron cyclotron emission using Fourier transform spectroscopy in Wendelstein 7-X*, 2020 *JINST* **15** P09024.

[24] L. Krier et al., *Theoretical investigation on possible operation of a 140 GHz 1 MW gyrotron at 175 GHz for CTS plasma diagnostics at W7-X*, *Phys. Plasmas* **27** (2020) 113107.

[25] L. Krier et al., *Short-pulse frequency stabilization of a MW-class ECRH gyrotron at W7-X for CTS diagnostic*, *Fusion Eng. Des.* **192** (2023) 113828.

[26] S. Ponomarenko et al., *Development of the 174 GHz Collective Thomson Scattering Diagnostics at Wendelstein 7-X*, to be published in *Rev. Sci. Instrum.* (2023).

[27] Y. Corre et al., *Thermographic reconstruction of heat load on the first wall of Wendelstein 7-X due to ECRH shine-through power*, *Nucl. Fusion* **61** (2021) 66002.

[28] D. Moseev et al., *Collective Thomson scattering diagnostic at Wendelstein 7-X*, *Rev. Sci. Instrum.* **90** (2019) 013503.

[29] A. Spanier et al., *Performance of the First Neutral Beam Injector at the Wendelstein 7-X Stellarator*, *Fusion Eng. Des.* **163** (2021) 112115.

2024 JINST 19 C03056